Katja Rademaker (Autor)

Rare Earth-Doped Alkali-Lead-Halide Laser Crystals of Low-Phonon Energy

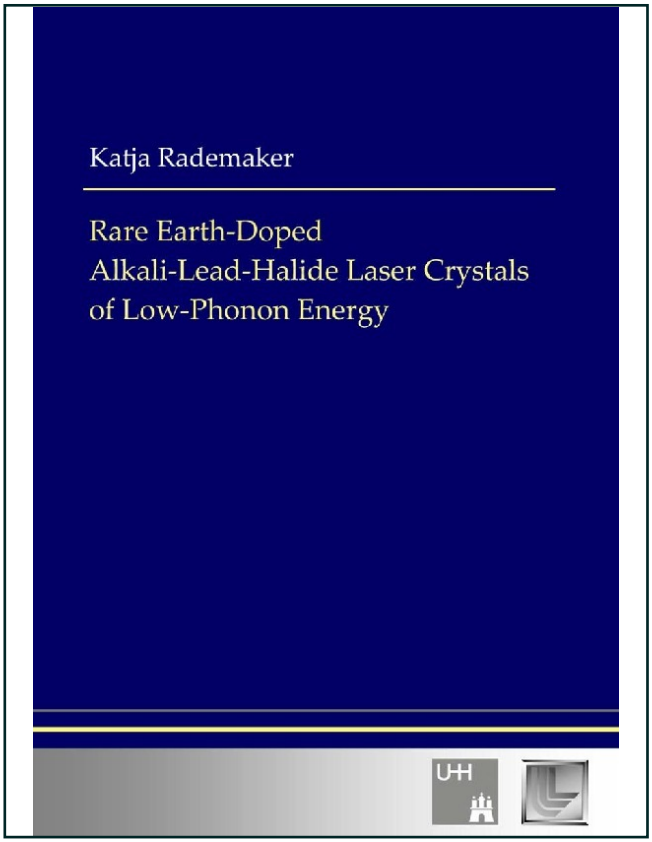

https://cuvillier.de/de/shop/publications/2358

1. Introduction

1.1 Motivation and Background

Long Wavelength Infrared (LWIR) Lasers are of great interest as beneficial sources for remote sensing in the vibrational fingerprint region (pollution monitoring), thermal scene illumination, and infrared spectroscopy in clinical and diagnostic analysis etc. Especially, broadly tunable LWIR laser sources can enable e.g. the detection of various gaseous species that arise both naturally and as by-products of our technological society (Figure 1-1). In particular solid-state lasers are feasible as coherent light sources, because of their compactness, efficiency, brightness, ease of deployment, reliability as well as low fabrication and maintenance costs. Here, rare earth ions as active dopants are advantageous since their energy level structure principally shows energy gaps in the LWIR region (Fig. 1-2) and they have absorption bands to pump the LWIR transitions directly with pump sources readily available on the market (such as diodes). The coverage of a broad wavelength region could in principle be possible with rare earth ions as indicated in Fig. 1-1.

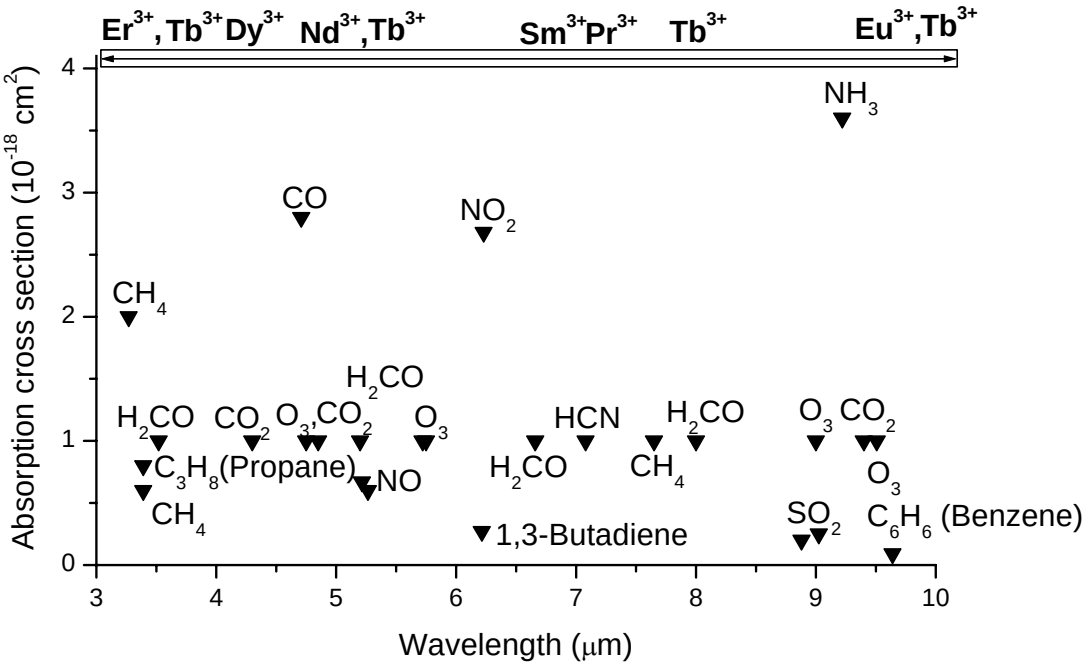

Fig. 1-1. *Absorption cross section of different gaseous species (based on data in [Mea82],[Pla65],[Pug76]). Rare earth-doped low-phonon energy laser host matrices could provide a way for the detection of e.g. pollution gases in the wavelength region 3-10 μm. Possible trivalent rare earth ions are indicated. Gas species of not clearly identified cross section are set to 1x10^{-18} cm^2.*

Currently, more complex and expensive systems such as optical parametric oscillators (OPOs) operate in the wavelength region of interest like e.g. one of the atmospheric transmission windows at ~ 8-13 µm (Appendix A, Fig. A-1). In this context other competitive coherent light sources such as gas lasers (like CO_2) and quantum-cascade (QC) diode lasers ([Fai94], [Bec03], [Pfl03]) have to be noted. However, they show limitations regarding e.g. tunability, efficiency, and/or average power.

Thus, mainly for the purpose mentioned above, herein the potential of rare earth-doped potassium-lead-bromide (KPb_2Br_5 or KPB) and rubidium-lead-bromide ($RbPb_2Br_5$ or RPB) crystals as new solid-state laser host materials is explored.

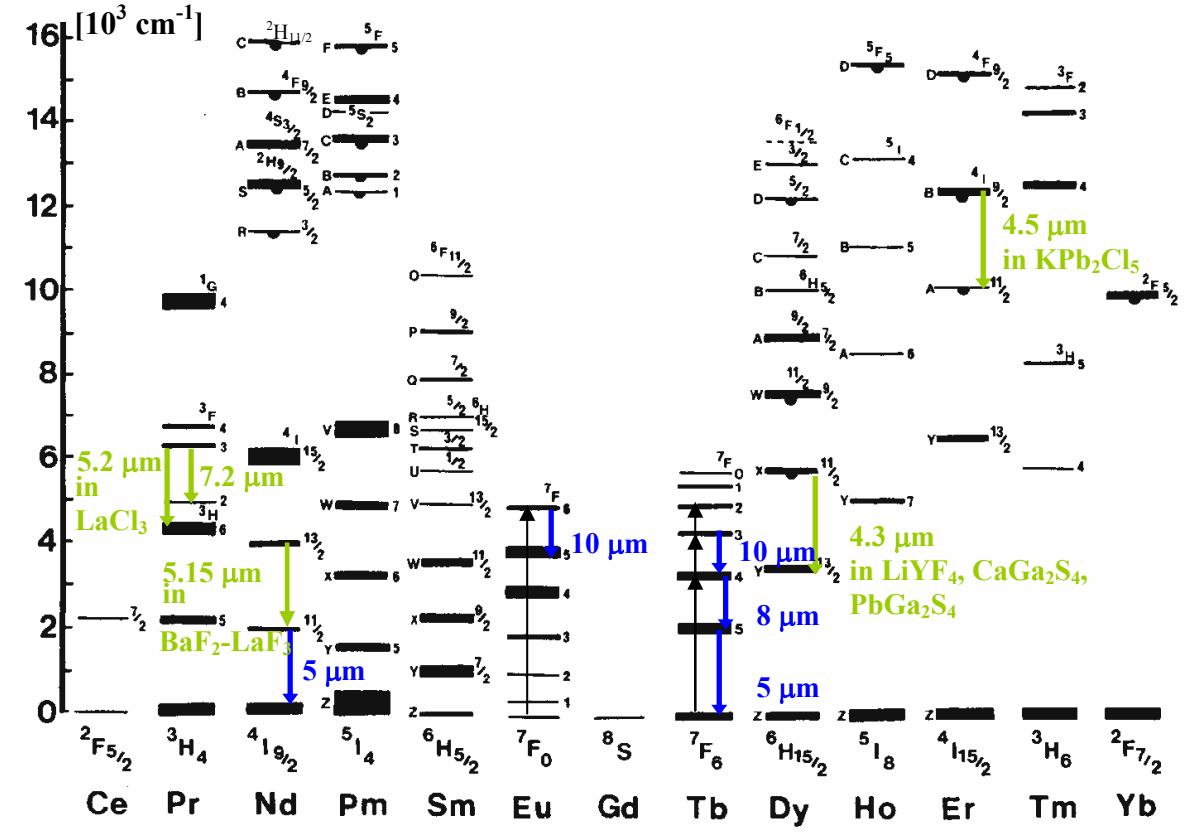

Fig. 1-2. *Energy level diagram of trivalent rare earth ions [Die68]: Room-temperature, solid-state laser transitions beyond 4 µm are rare (green) ([Bow96], [Nos99], [Bow01],[Bas05], [Kam96]). Thus, the investigation of rare earth-doped low-phonon energy host matrices could reveal further (mainly directly pumpable) LWIR laser transitions as indicated (blue) for some transitions of the RE^{3+} ions of this study.*

To achieve acceptable quantum efficiency from a given energy level a rule of thumb demands that at least four to six (maximal energy) phonons span the energy gap to the next lowest level. Otherwise the luminescence is quenched, as it is typical for most fluorides and oxides emitting at wavelengths longer than 4 µm (with maximum phonon energies in excess of

500 cm^{-1}). Solid state lasers beyond 4 μm at room temperature are indicated in Fig. 1-2. As can be seen, laser transitions in the long wavelength region are still rare. Until now the longest laser wavelength in a solid state laser material at room temperature (7.2 μm, Figure 1-2) has been achieved with the low-phonon energy host lanthanum chloride ($LaCl_3$) doped with Pr^{3+} [Bow96]. This chloride host has the disadvantage of being highly hygroscopic, and somewhat impractical. So, it was an important step towards practicality when potassium-lead-chloride (KPb_2Cl_5 or KPC) was identified as a moisture-resistant, low-phonon energy host for mid-IR-applications ([Pag97], [Nos98], [Isa98], [Tka99a], [Tka99b]). In KPC laser operation has been achieved with the rare earth ions Nd^{3+} (1.06 μm) [Nos00a], Dy^{3+} (2.43 μm) [Nos99], and Er^{3+} (1.7 μm, 4.5 μm (Fig. 1-2)) [Bow01].

Further spectroscopic investigations of RE^{3+}-doped KPC crystals have been performed with Pr^{3+} ([Bal02], [Tka02a], [Bal03a], [Bas02]), Nd^{3+} ([Tka02a], [Jen01], [Bas02], [Jen02], [Tka02b]), Tb^{3+} ([But02], [Tka02a]), Er^{3+} ([Tka02a], [Jen03], [Tka03], [Roy03]), Dy^{3+} ([Nos01], [Tig01]), and Ho^{3+} [Tka02a] as well as for doubly-doped systems like Pr^{3+}, Yb^{3+} [Bal03b] and Tb^{3+}, Tm^{3+} [Okh03] in order to evaluate the possibilities of long wavelength laser transitions and to study energy transfer mechanisms and upconversion of this low-phonon energy host material.

The alkali-lead-halide host crystals KPB and RPB reported in this study evidence similar properties to KPC (incorporate rare earth ions, moisture-resistant, transparent in the wavelength region of interest etc.), but with the added advantage of even lower phonon energies (because of the higher mass of the vibrating bromine constituent) with values of ~ 140 cm^{-1} (section 3.1). The vibrational energy is most simply described by

$$\bar{\nu}_{vibr}=(k/\mu)^{1/2}, \qquad (1\text{-}1)$$

where k is an effective force constant and μ is the reduced mass of the vibrating constituents. Therefore, the phonon energy is roughly expected to be ~ 1.5x smaller as one passes the periodic table from chloride to bromide anions. This will minimize the nonradiative decay due to multiphonon interactions, in principle permitting lasing at new wavelengths, e.g. in the LWIR region (perhaps as long as 10 μm), since electronic states which are immediately depleted in oxides and fluorides become metastable. For the same reason new pathways for upconversion lasing can occur.

Here, main focus is on the spectroscopic investigation of Nd^{3+}-doped KPB and RPB as well as Tb^{3+}- and Eu^{3+}-doped KPB with respect to its potential as a new solid state laser material. For example this could mean the possibility of the achievement of LWIR lasing up to 10 μm

in wavelength with dopant ions like Tb^{3+} for example (Fig. 1-2) and also lasers operating at new wavelengths e.g. in the visible or near infrared (e.g. 1.2 µm for Nd-doped MPb_2Br_5 (M=K, Rb)). Laser operation of the latter one will actually be presented in this study. A few of the investigated transitions and processes presented and further described in the following study are illustrated for the rare earth ion Nd^{3+} in Fig. 1-3. This includes emission (EM), excited state absorption (ESA), energy transfer upconversion (ETU), reabsorption (RA), lasing (⇝), and cross relaxation (CR) as well as the influence of multiphonon relaxation (MPR). Ground state absorption (GSA) is not displayed in the figure.

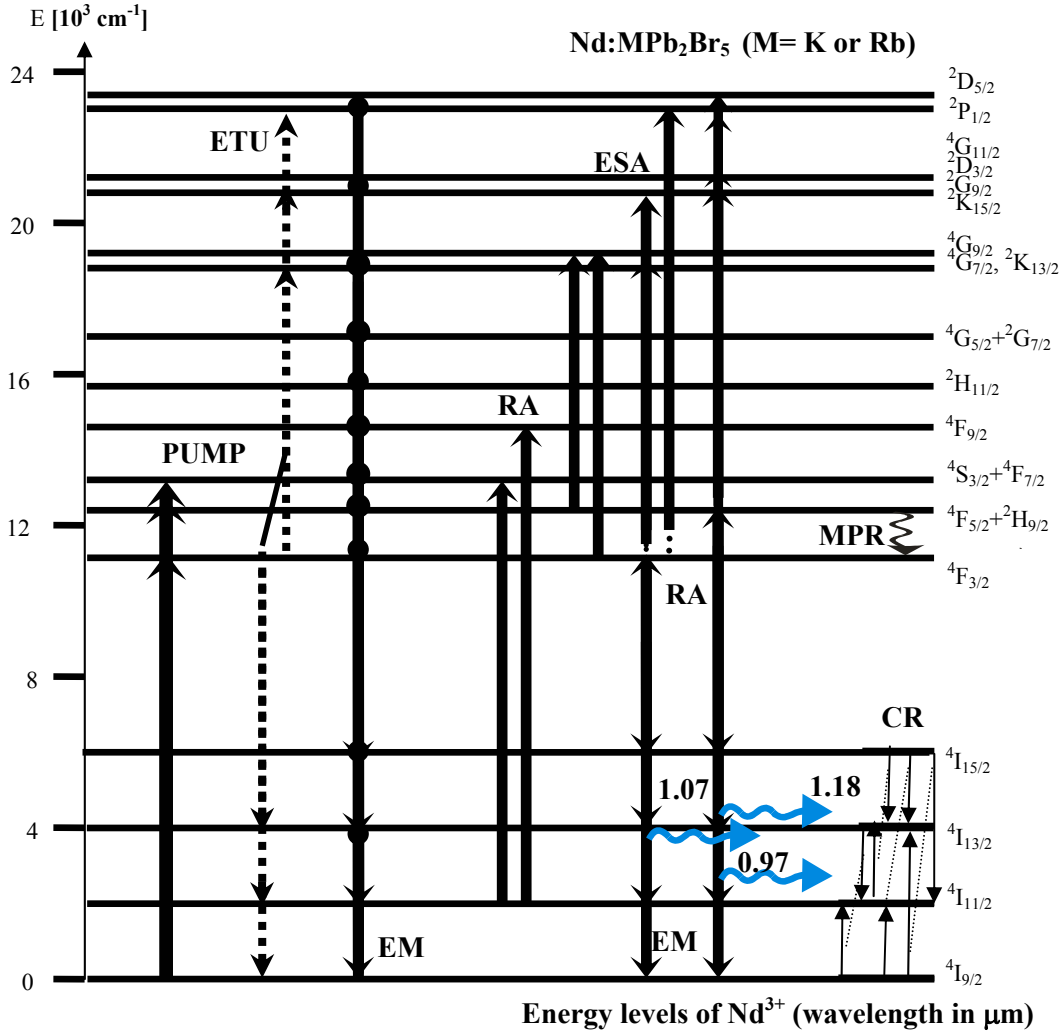

Fig. 1-3. *For illustration, the energy level diagram of Nd:MPB (M= K or Rb) displays some pumping and emitting levels of this study. Laser activity (⇝) will be presented for the first time in moisture-resistant, bromide host crystals of low-phonon energy, also at new wavelengths (with Nd:RPB) for the first time in any crystal. Some of the discussed transitions based on processes such as emission (EM), excited state absorption (ESA), energy transfer upconversion (ETU), cross relaxation (CR), reabsorption (RA), and multiphonon relaxation (MPR) are also indicated. The measured ground state absorption (GSA) and pumping into higher lying levels is not included.*

During the course of this study spectroscopic investigations on the KPB host crystal doped with Er^{3+} and Nd^{3+} have also been presented by Hoemmerich et al. ([Hoe04], [Hoe05]).

This work is structured in 4 chapters. The following section of this first chapter gives a brief overview of the most important theoretical aspects of this thesis. The preparation including crystal growth and physical properties of the rare earth-doped bromide crystals as well as experimental methods used in this study are described in chapter 2.

The results of the spectroscopic investigation and laser operation are described and discussed in chapter 3. The first section of this chapter states the low-phonon energy of the investigated bromide crystals in comparison to other host materials. As a result, nonradiative (multiphonon) decay competes less effectively with the radiative decay in the investigated bromide materials compared with e.g. the chloride analogs as described in section 3.2. Here, the study of slow nonradiative decay includes absorption spectra, emission spectra, emission lifetimes recorded for Nd^{3+}-, Tb^{3+}- and partly Eu^{3+}-doped MPb_2Br_5 (M=Rb, K) samples at room temperature as well as calculations of cross sections, Judd-Ofelt parameters, radiative transition probabilities for relevant (laser) transitions, and multiphonon decay rates.

Nonradiative decay like e.g. multiphonon emission is a temperature dependent process. Thus, temperature dependent quenching is investigated in section 3.3 for long wavelength transitions of Tb^{3+}-doped KPB samples including an approach to fit the temperature dependency of the decay. This provides a way to evidence the energy (and number) of phonons involved in the process which will be compared with the results stated in previous sections. In this context emission from the potential 10 μm emitting level in Tb^{3+}-doped KPB is investigated. Multiphonon fitting parameters characteristic for the host material are also obtained. Low temperature spectroscopy for Nd^{3+}-doped KPB will be presented in section 3.4 where the main purpose was to determine the Stark levels. This is beneficial e.g. for the determination of transition wavelengths which are particularly used in following sections about optical pump-probe processes and upconversion.

Laser results obtained from rare earth-doped KPB and RPB samples will be given in section 3.5. Here, laser activity resulting from new transitions in Nd^{3+}-doped bromide samples is presented which makes also lasing e.g. in the long wavelength-IR region with these materials promising. The main purpose of the study in section 3.6 is to gain further insights into the lasing potential of Nd^{3+} in RPB and KPB, especially for the new laser wavelengths stated in the previous section. Cw pump-probe spectra are presented in order to discuss excited state absorption (ESA) and reabsorption processes (RA) due to the long lived lower laser levels competing with gain, as well as possible depopulation mechanisms feasible for more efficient

laser operation in these bromide crystals. Line strengths of induced electric dipole and of magnetic dipole transitions and effective cross sections of ESA and RA transitions competing with the (laser) emission transitions, as well as cross relaxation (CR) processes among the lower laser levels, will be given. For comparison pump-probe spectra will also be presented for the potassium-lead-chloride host (Nd^{3+}:KPC). The presence of upconversion as illustrated for Nd^{3+}-doped KPB in section 3.7 could lead in principle to the possibility of upconversion lasing. In chapter 4 the results are summarized.

1.2 Theoretical Aspects

In this section a brief overview of the most important theoretical aspects will be presented accompied by references for a detailed study.

1.2.1 Energy Splitting of Trivalent Rare Earth Ions

The active dopant ions Nd^{3+}, Eu^{3+}, and Tb^{3+} discussed in this study are trivalent lanthanide ions. Their electron configuration is given by [Xe]$4f^3$ (Nd^{3+}), [Xe]$4f^6$ (Eu^{3+}), and [Xe]$4f^8$ (Tb^{3+}), respectively [Hoe79].[1] One characteristic is the unfilled 4f shell, which is shielded by the closed $5s^2$ and $5p^6$ Xenon [Xe] orbitals as often represented in the literature by the radial charge distribution of the electrons as a function of the distance to the nucleus [Wyb65]. Therefore, the influence of the crystalline field can be treated as an external small perturbation of the free ion Hamiltonian as described in [Hen89] and the linewidth of the luminescence transitions in the 4f shell of RE^{3+} (RE=rare earth) ions is usually smaller than for transition metals or 4f↔5d transitions of RE^{3+} ions where the electron-phonon coupling is stronger. The configuration coordination model [Hen89] and the ligand-field theory ([Sch80], [Sch73]) explain these differences.[2] Line broadening of the 4f transitions can occur if e.g. the rare earth ion is incorporated on various sides of the crystalline host, if there are crystal defects present etc. [Hen89].

The splitting of the energy and their degeneracy is illustrated in Figure 1-4 indicating the influence of the different Hamilton operators involved (as further described in Henderson&Imbusch [Hen89]). Here, as well as in the energy level schemes shown for the different active dopant ions in following sections (Figs. 3-3, 3-7, 3-11) the different states are indicated after Russell-Sanders coupling (LS-coupling), where the sum of total orbital momentum $\vec{L} = \sum_i \vec{l}_i$ and total spin momentum $\vec{S} = \sum_i \vec{s}_i$ of all electrons i is added to form the total angular momentum $\vec{J} = \vec{L} + \vec{S}$ [Sch88]. Note, that in the case of approximately equal

[1] [Xe]-electron configuration:$1s^2 2s^2 2p^6 3s^2 3p^6 3d^{10} 4s^2 4p^6 4d^{10} 5s^2 5p^6$
[2] also described in the authors diploma thesis [Rad00]

quantity of Coulomb interaction and spin-orbit coupling term, mixing of different LS-states with the same quantum number J appears and therefore, the free ion states are actually linear combinations of different LS-states, so called intermediate coupling [Con70].

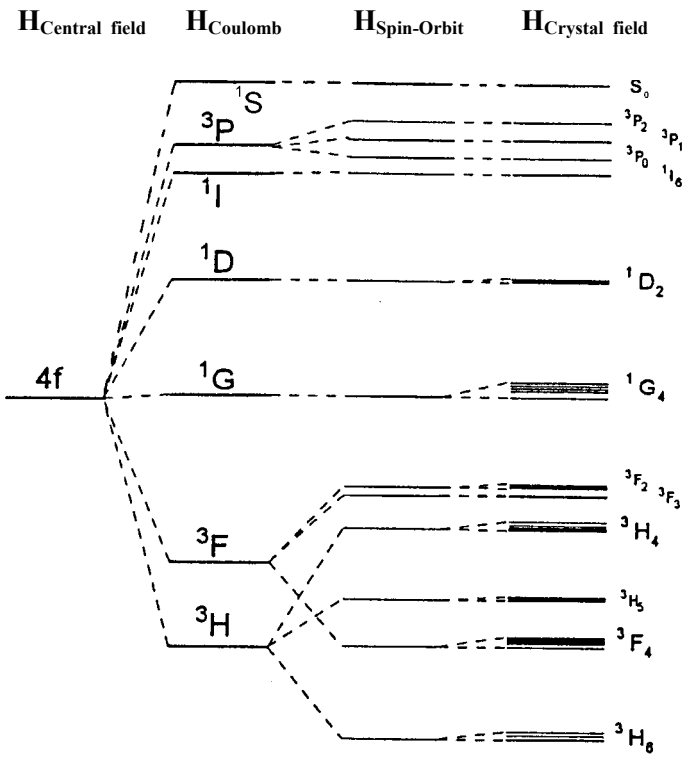

Term	$4f^n$	^{2S+1}L	$^{2S+1}L_J$	Γ_i
Degeneracy	$\binom{14}{12} = 91$	(2L+1)(2S+1)	(2J+1)	Depends on crystal field symmetry
Energy splitting	~10^4-10^5 cm^{-1}	~10^3-10^4 cm^{-1}	~10^3-10^4 cm^{-1}	~10^2-10^3 cm^{-1}

Fig. 1-4: *Energy splitting of Tm^{3+}:YAG ($4f^{12}$) [Gru89].*

The state wavefunctions in the intermediate coupling scheme are most clearly distinguished by using group theory or rather irreducible representations of the group constructed by using tensor operators as shown by Racah [Rac42]. For a detailed study of the classification of f^n configurations (using group theory) see also Judd [Jud63] and Wybourne [Wyb65]. After Kramer's rule, the number of Stark levels is doubly degenerated for an odd number of electrons, rescinded in the presence of a magnetic field.

1.2.2 Radiative Transitions

In this section the most important formulas used to calculate the radiative transition probabilities will mainly be stated. For a detailed study on the theoretical aspects given in this section the following references should be cited: Carnall&Crosswhite [Car77],